Rapid Convective Transport of Tropospheric Air into the Tropical Lower Stratosphere during the 2010 Sudden Stratospheric Warming

Eguchi Nawo, Kodera Kunihiro, Beatriz M. Funatsu, Takashima Hisahiro, Rei Ueyama

Rapid Convective Transport of Tropospheric Air into the Tropical Lower Stratosphere during the 2010 Sudden Stratospheric Warming

Nawo Eguchi[1], Kunihiko Kodera[2], Beatriz M. Funatsu[3], Hisahiro Takashima[4], and Rei Ueyama[5]

[1]*Research Institute for Applied Mechanics, Kyushu University, Fukuoka, Japan*
[2]*Institute for Space-Earth Environmental Research, Nagoya University, Nagoya, Japan*
[3]*LETG-Rennes COSTEL, CNRS UMR 6554, Université de Rennes 2, Rennes, France*
[4]*Faculty of Science, Fukuoka University, Fukuoka, Japan*
[5]*NASA Ames Research Center, Moffett Field, CA, USA*

Abstract

A possible transport mechanism from the tropical troposphere to the lower stratosphere (LS) across the tropical tropopause layer (TTL) is through convective overshooting clouds (COV) that inject air with tropospheric characteristics (high carbon monoxide (CO) and low ozone (O_3) concentrations) into the LS over a few days. Evidence of such convective intrusions was observed at the end of January 2010, associated with increased convective activity over the southern African continent following the onset of a sudden stratospheric warming (SSW) in the northern hemisphere, lasting approximately two weeks. The modulation of tropical stratospheric upwelling by SSW appears to have forced stronger and deeper tropical convection, particularly in the Southern Hemisphere tropics. The tropospheric (CO-rich, O_3-poor) air injected into the TTL by COV then gradually moved upward via the tropical stratospheric upwelling strengthened by SSW. Meanwhile the O_3 decrease started in the middle stratosphere and descended gradually to the TTL, indicating that the effect of stratospheric upwelling reached the TTL. The present results suggest that the direct and indirect (strengthened convective clouds) effects of stratospheric upwelling modulated by SSW can have a large impact on the trace gas fields in the TTL and LS.

(**Citation**: Eguchi, N., K. Kodera, B. M. Funatsu, H. Takashima, and R. Ueyama, 2016: Rapid convective transport of tropospheric air into the tropical lower stratosphere during the 2010 sudden stratospheric warming. *SOLA*, **12A**, 13−17, doi:10.2151/sola.12A-003.)

1. Introduction

Tropical stratospheric upwelling has been shown to vary on seasonal and interannual timescales, the latter driven by well-known phenomena such as the Quasi-Biennial Oscillation (QBO), which impacts the lower stratospheric temperature (Collimore et al. 2003; Ueyama et al. 2013) and concentrations of trace gases, such as carbon monoxide (CO) and ozone (O_3) (Abalos et al. 2012, hereafter A12). Additionally, sporadic events such as sudden stratospheric warming (SSW) enhance the tropical stratospheric upwelling, which in turn affects temperature perturbations in the tropical lower stratosphere (LS) and Tropical Tropopause Layer (TTL) (Kodera 2006; Eguchi and Kodera 2010).

The stratospheric circulation changes associated with SSW not only modulate the temperature in the TTL but also increase both cirrus cloud amounts and tropical convective activity, and modify the general circulation in the troposphere (e.g., Eguchi and Kodera 2007, 2010; Kodera et al. 2011; Eguchi et al. 2015 (hereafter E15); Kodera et al. 2015 (hereafter K15); Evan et al. 2015). E15 found that SSW-induced stratospheric upwelling increases deep convective activity by decreasing the stability in the TTL.

A12 showed that the upwelling rate (more precisely, residual vertical velocity) in the tropical LS correlates well with CO and O_3 on seasonal and sub-seasonal scales. Many studies have focused on the Asian and North American monsoons in boreal summer, and found that monsoon circulation and the deep convective transport across the upper troposphere (UT)/LS play an important role in the CO distribution in LS, (e.g., Park et al. 2007; Randel et al. 2015). However, few studies have focused on the intra-seasonal variations of trace gases in the tropical UT/LS during boreal winter (BW) (e.g., Wang et al. 2014).

Figure 1 shows time series of 30-day running means of CO at 68 hPa and vertical velocity (w) converted from pressure velocity at 100 hPa averaged over the tropics from 2008 to 2012. The seasonal cycle of CO in LS has its maximum in BW and minimum in boreal fall (A12; Minschwaner et al. 2016). Both variables increased nearly simultaneously in the 2010 BW when the lowest tropical LS temperature and the strongest upward velocity recorded by the Earth Observing System (EOS) Microwave Limb Sounder (MLS) in the period 2004−2015 were observed. Note that the CO and stratospheric upwelling were well correlated in 2010 but not as well in other years; tropospheric CO distribution is fairly constant from year to year. These inter-annual variations are discussed in Section 4.

In addition to the influence of stratospheric upwelling, changes in tropical general circulation and convective activity have the potential to affect the concentration of various tracers in the UT/LS. Air with tropospheric characteristics (CO-rich and O_3-poor) may be injected into LS by convective overshooting clouds (COV) within a few days. The increase in CO at the end of January 2010, concurrent with the increase in stratospheric upwelling (Fig. 1),

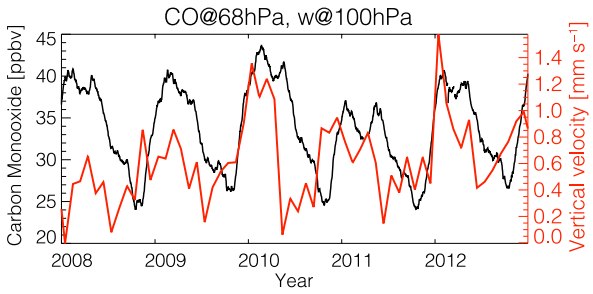

Fig. 1. Time series of 30-day running means of zonal mean CO [ppbv] at 68 hPa averaged between 17.5°S and 17.5°N (top), and vertical velocity (w) [mm s^{-1}] at 100 hPa averaged between 15°S and 15°N (bottom). The w is converted from pressure velocoty [Pa s^{-1}] of ERA-Interim reanalysis and the CO data are from the Earth Observing System (EOS) Microwave Limb Sounder (MLS).

Corresponding author: Nawo Eguchi, Research Institute for Applied Mechanics (RIAM), Kyushu University, Kasuga Park 6-1, Kasuga, Fukuoka 816-8580, Japan. E-mail: nawo@riam.kyushu-u.ac.jp.

may have been influenced by the SSW-induced changes in tropical convection and tropospheric circulation. We therefore focus on this two-week period around the SSW when the influences of stratospheric upwelling and tropical convection on CO and O_3 fields in the LS are clearly observed.

2. Analysis data

We use CO, O_3, ice water content (IWC) and water vapor (WV) data measured by the EOS/MLS (Level−2, ver.4.2x) (Livesey et al. 2015) at pressure levels between 215 and 68 hPa in the UT/LS. Daily data on 2.5° latitude × 2.5° longitude grid were derived from the orbital data. CO and O_3 are treated as tropospheric and stratospheric tracers, respectively. Analyzing the variations of both species clearly illustrates the stratosphere-troposphere air exchange. Note that the current version (ver.4.2x) of the CO data reduced the artifacts induced by cloud compared to the previous version (ver.3.3x), and the cloud screening was taken based on Livesey et al. (2015).

To isolate the deep convective effect on the trace gases, we use deep convective cloud (DC) and COV are that detected using the Microwave Humidity Sensor (MHS) channels 3 to 5, on the basis of the brightness temperature depression due to ice particles in precipitating clouds. The details of the DC and COV detection method are found in Hong et al. (2005) and Funatsu et al. (2012). We use MHS data from NOAA18 and MetOp-A; the equatorial crossing time for these platforms was approximately 14:00 local time (LT) for NOAA18 (in 2010), and 21:30 LT for MetOp-A. The original, irregularly sampled data were first regridded on a 0.25° latitude × 0.25° longitude grid. Next, the DC and COV occurrences were resampled to a grid of 2.25° latitude × 2.25° longitude for plotting purposes.

Cloud fraction [%] data are derived from the Cloud Layer Product (Level−2, ver.3.01) of the Cloud-Aerosol LIdar with Orthogonal Polarization (CALIOP) (Winker et al. 2007). Daily meteorological parameters, such as temperature, meridional and vertical wind fields, were obtained from the ERA-Interim reanalysis (Dee et al. 2011). We use data on pressure levels between 1000 hPa and 30 hPa (levels in the TTL and LS are 150, 125, 100 and 70 hPa) with a horizontal resolution of 1.5° latitude × 1.5° longitude.

3. Results

Figures 2a and 2b show the daily time series of the zonal mean heat flux ($\overline{v'T'}$) at 100 hPa averaged over the northern middle latitudes (45°N−75°N) and the tendencies of temperature ($\partial T/\partial t$) at 100 hPa averaged over the southern tropical region (20°S−0°) from 10 January to 10 February, 2010. The $\overline{v'T'}$ at 100 hPa indicates planetary waves propagating from the troposphere to the stratosphere in the middle latitudes. The $\partial T/\partial t$ at 100 hPa is well correlated with the changes in w at 100 hPa (E15; K15); these parameters represent the strength of the stratospheric meridional circulation. The $\overline{v'T'}$ increased in mid January (Fig. 2a), which led to a cooling in the tropics (Fig. 2b) and warming in the polar region (Fig. 1 of E15). The lowest $\partial T/\partial t$ at 100 hPa appeared around 25 January coincident with the maximum of $\overline{v'T'}$.

Figures 2c and 2d show the time series of the tendencies of O_3 ($\partial O_3/\partial t$) and CO ($\partial CO/\partial t$) at 100 hPa. The $\partial O_3/\partial t$ decreased gradually after 20 January, following the enhanced upwelling at 100 hPa as seen in $\partial T/\partial t$. In particular, after 25 January, the area of negative $\partial O_3/\partial t$ spread below 100 hPa, and reached 177 hPa around 1 February (Fig. 2e). Vertical velocity varied similarly (Fig. 2g). Below 100 hPa, the area of negative $\partial O_3/\partial t$ ascended between 20 and 25 January. These features suggest that there are both tropospheric and stratospheric effects of SSW on the O_3 field.

On the other hand, $\partial CO/\partial t$ at 100 hPa peaked around 25 January when the $\overline{v'T'}$ was at its maximum and $\partial T/\partial t$ was the lowest, and $\partial CO/\partial t$ peaked again on 2 February (Figs. 2d and 2f), reflecting the change in tropospheric upwelling (Fig. 2g). The

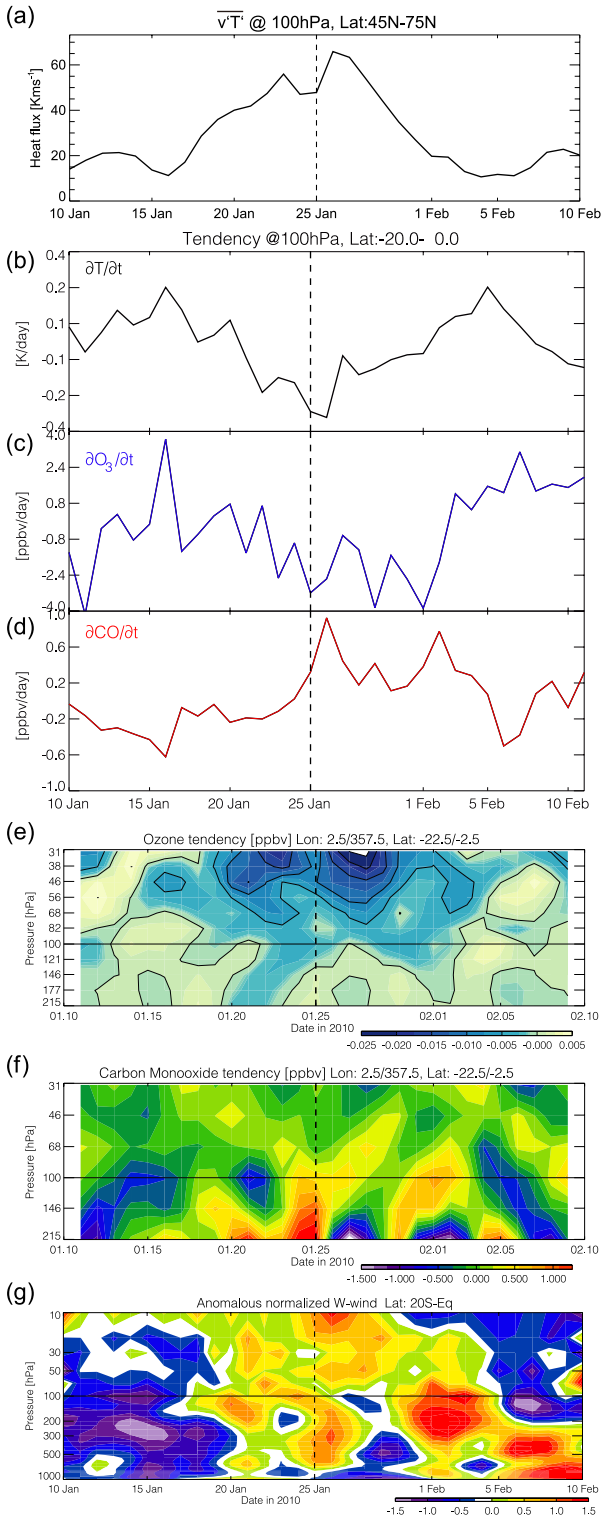

Fig. 2. Time series from 10 January to 10 February, 2010 of (a) zonal mean eddy heat flux ($\overline{v'T'}$) [K m s^{-1}] at 100 hPa averaged between 45°N and 75°N and (b, c and d) zonal mean temperature, and O_3 and CO tendencies per day ($\partial T/\partial t$, $\partial O_3/\partial t$, $\partial CO/\partial t$) at 100 hPa averaged between 20°S and 0°. (e, f and g) Time-pressure sections of 3-day running means of zonal mean O_3 and CO tendencies ($\partial O_3/\partial t$ and $\partial CO/\partial t$) [ppbv day^{-1}] and vertical velocity [m s^{-1}] averaged between 20°S and 0°. The 3-day running mean was applied at each pressure level. The pressure range is between 215 hPa and 31 hPa for (e and f) and between 1000 hPa and 10 hPa for (g). The vertical velocity was normalized by the average from 10 January to 10 February at each level. The horizontal line in (e, f and g) corresponds to the 100 hPa pressure level. The vertical dashed lines of all panels indicate 25 January 2010, the key-date.

∂T/∂t became negative around 20 January, after which upward velocity in the southern tropics strengthened in the troposphere and stratosphere (Fig. 2g). The upward motion in the stratosphere continued until the beginning of February, and strengthened in the troposphere around 25 January and 1 February. This suggests that the enhancement of tropical stratospheric upwelling following the SSW destabilized the TTL (E15 and K15) and enhanced convection (Fig. 2g, where w is used as a proxy for convective updraft), as shown in E15 and K15.

The peaks in ∂CO/∂t at 100 hPa were evident throughout the UT (at 215 and 146 hPa) around 25 and 30 January (Fig. 2f) and the CO increase occurred at the same time as the enhancement in w (Fig. 2g). The rapid vertical transport of CO into the TTL shown in Fig. 2f is observed chiefly over the African sector where the main source of CO due to biomass burning is located, and where COV activity was enhanced after the SSW event. In the present study, 25 January is defined as the key-date when the CO at 100 hPa began to increase.

The positive ∂CO/∂t propagated upward gradually from the TTL to the LS after the key-date. The upward speed in the LS based on CO was approximately −10 hPa/day (~0.8 cm/sec) averaged between 100 and 50 hPa in the southern tropics (20°S−0°), which is approximately three to six times faster than the maximum vertical velocity of the residual circulation (w*) in the southern tropics at the end of January 2010 (0.25 (0.13) cm/sec at 100 (70) hPa levels; M. Abalos, personal communication). The difference in speed could be due to horizontal mixing and/or some disturbance (e.g., convection) on the sub-grid scale, coarse vertical resolution of MLS observation and vertical diffusion. On the other hand, the negative $\partial O_3/\partial t$ feature propagated downward from the middle stratosphere (MS) to the TTL at a speed consistent with the w* distribution (not shown). The enhancement of tropical stratospheric upwelling associated with SSW began in the MS and descended gradually to lower levels, and both $\partial O_3/\partial t$ and ∂CO/∂t in the LS were strongly affected by the enhanced tropical stratospheric upwelling.

Figure 3 shows the differences between the averages over eight days before and after the key-date (25 January–1 February minus 17−24 January). The CO at 100 hPa (Fig. 3b) increased over Africa, the eastern Indian Ocean and the central Pacific, whereas O_3 at 100 hPa (Fig. 3c) decreased throughout the tropics, with strong minima seen notably over the central southern Pacific and northwest Australia in particular. The IWC difference distribution at 100 hPa (Fig. 3d) shows that regions of high occurrence of ice cloud were seen over southeastern Africa, South America, the central Pacific, and northern Australia. This distribution is closer to that of the CO difference at 68 hPa than that at 100 hPa, suggesting that the CO at 68 hPa, O_3 at 100 hPa, and IWC at 100 hPa are closely related with the stratospheric upwelling distribution, which distributed them zonally. In contrast, the CO distribution at 100 hPa retained the tropospheric zonal asymmetry of the biomass burning source regions. The WV field at 100 (146) hPa (not shown) exhibits dry (wet) regions in the presence of ice clouds, which means that UT was hydrated by deep convection (Fig. 3e) whereas the cooling associated with stratospheric upwelling dehydrated the region with TTL cirrus.

Figure 4 focuses on the changes in COV and CO around the key-date over southern Africa, because Africa is the main source of CO and variation of zonal mean CO field at LS were found. The CO was enhanced over the central Pacific, off the west coast of Australia and west coast of South America, but the direct effect

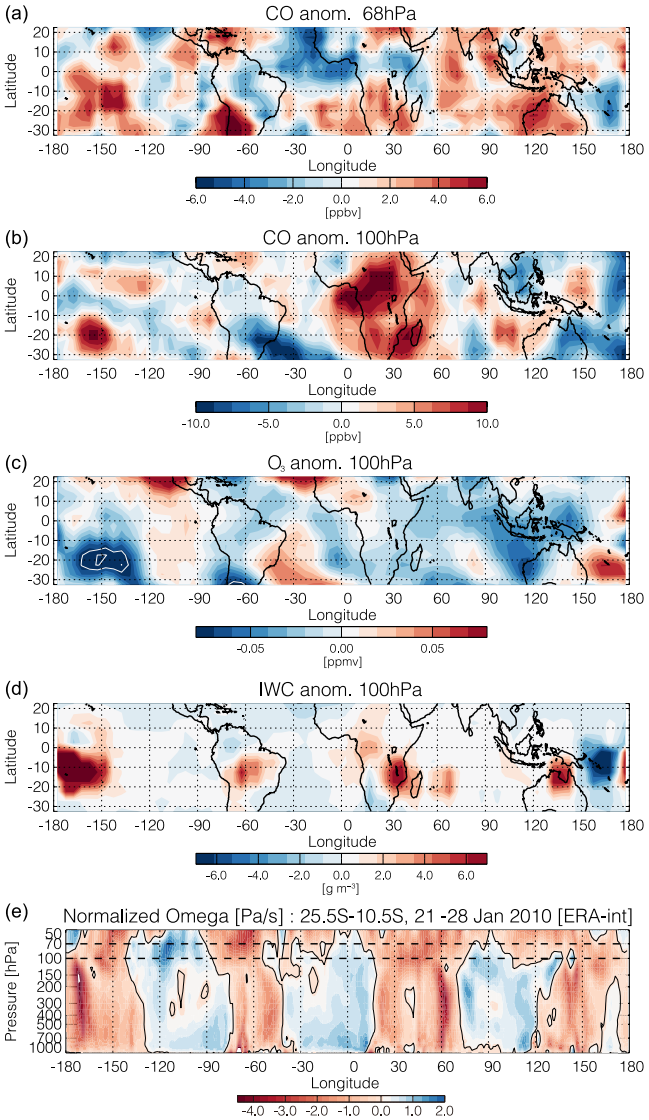

Fig. 3. Maps of differences in CO [ppbv] between 17−24 January and 25 January–1 February at (a) 68 and (b) 100 hPa, (c) O_3 [ppmv], and (d) ice water content (IWC) [g m^{-3}] at 100 hPa. (e) The longitude-pressure section of normalized vertical pressure velocity [Pa s^{-1}] averaged between 25.5°S and 10.5°S, 21 and 28 January, 2010. The normalization is with respect to the standard deviation at each pressure level. The horizotal dashed lines indicate 100 and 70 hPa.

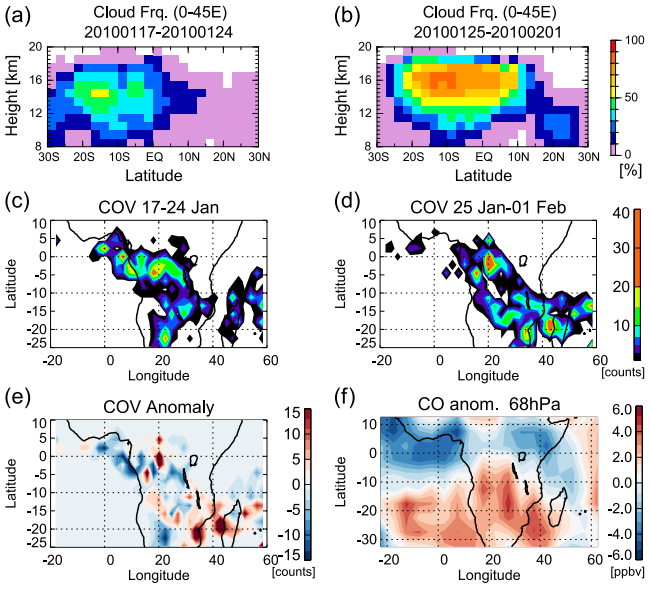

Fig. 4. (top: a and b) Latitude-height sections of cloud fraction [%] over Africa (0°E−45°E). (middle: c and d) Maps of COV [counts] over southern Africa. Left panel is 17−24 January and right panel is 25 January−1 February, 2010. (bottom: e and f) Difference maps of COV and CO [ppbv] at 68 hPa between the periods 17−24 January and 25 January−1 February.

by COV, such as the rapid transport from the lower troposphere (LT) to the TTL, was seen only over Africa. Over southern Africa, the cloud frequency above 17 km increased significantly after the key-date (Figs. 4a and 4b). The cloud top height also increased, with the most frequent altitude increasing from 14 to 16 km. In Figs. 4c and 4d, the COV became relatively more widespread and enhanced around 20°E just south of the equator, and around the southeastern coast of Africa and the west coast of Madagascar (30°E–40°E, 25°S–20°S) (Fig. 4e). In other words, the COV became active over southern Africa. It is argued that the effects of stratospheric upwelling located towards the Southern Hemisphere, were twofold: (i) cooling of the tropical UT/LS, and (ii) decrease in static stability causing deep convection to reach higher altitudes. The CO at 68 hPa increased over southern Africa and its vicinity (20°W–50°E) where the COV were also enhanced (Figs. 4f and 4e), suggesting that CO-rich air was transported vertically from LT via COV and then ascended via the stratospheric upwelling within one week.

Figure 5 shows maps of CO differences over three periods – the first period of which shown for reference– from the end of January to the beginning of February at 68, 100, and 215 hPa, corresponding to the LS, TTL, and UT, respectively. In the second period when the convection began to strengthen over Africa (Figs. 4d and 4e), the CO increased at 215 hPa mainly around the equator and increased at 100 hPa around the Mozambique Channel as well as over the equatorial region. In the third period, the CO at 215 hPa decreased, while that at 68 hPa increased especially over southeastern Africa and Madagascar. The CO at 100 hPa increased slightly. These features show that the CO-rich air was transported vertically over a period of a few weeks, except for the rapid transport into the TTL and LS via COV around the Mozambique Channel.

4. Summary and discussions

The present study examined the impact of stratospheric circulation change on trace gas fields (CO and O_3) in the TTL and LS during a SSW period. Trace gases in the TTL and LS were affected by both direct and indirect effects of stratospheric upwelling; SSW-induced upwelling (direct effect) and deep convection (indirect effect), the latter associated with the cooling and increase of instability in the TTL (E15). Our results suggest that in the short term, the enhancement of COV can have a large impact on the zonally averaged tracer fields in the tropical LS as shown in Fig. 1 and Fig. 2.

The main source of CO is in the LT especially over the equatorial Africa due to biomass burning during BW (Kopacz et al. 2010). The modeling study of Ott et al. (2011) showed that deep convection affects the CO distribution in the UT not only over regions of high CO concentration but also globally. The present results show an enhancement of CO at 68 and 100 hPa over southeastern Africa, which means that deep convection enhanced by the stratospheric upwelling transports CO-rich air from LT to TTL rapidly and directly regardless of the CO distribution in the LT.

Although there is downward motion around COV at the cloud top altitude, the total effect of COV on the transport of air mass is upward, which only lasts for about a day (e.g. Chaboureau et al. 2007). Our results show that, once the CO-rich air is injected by COV into TTL, the air propagates upward with the speed of w* modulated by SSW, which can be faster than the climatological mean upward velocity; approximately 0.04 cm/sec at 18 km (e.g., Schoeberl et al. 2008). The enhanced stratospheric upwelling then keeps the CO-rich tropospheric air ascending during the SSW period.

The O_3 field was also affected by both mechanisms; the tropospheric injection of O_3-poor air and stratospheric upwelling modulated by the SSW. The enhanced upwelling throughout the SSW period appeared to have forced the negative $\partial O_3/\partial t$ region to ascend in the UT (driven by convection) before the key-date, and the area of negative tendency to spread downward from MS to TTL. The O_3 variations were opposite to those of CO in LS/UT (50–215 hPa) after the key-date (Figs. 2c, 2d, 2e, and 2f). The lack of the relationship between CO and O_3 near 30 hPa is likely due to a source of CO in the upper stratosphere, which leads to a change in the gradient of CO in MS. The stratospheric upwelling

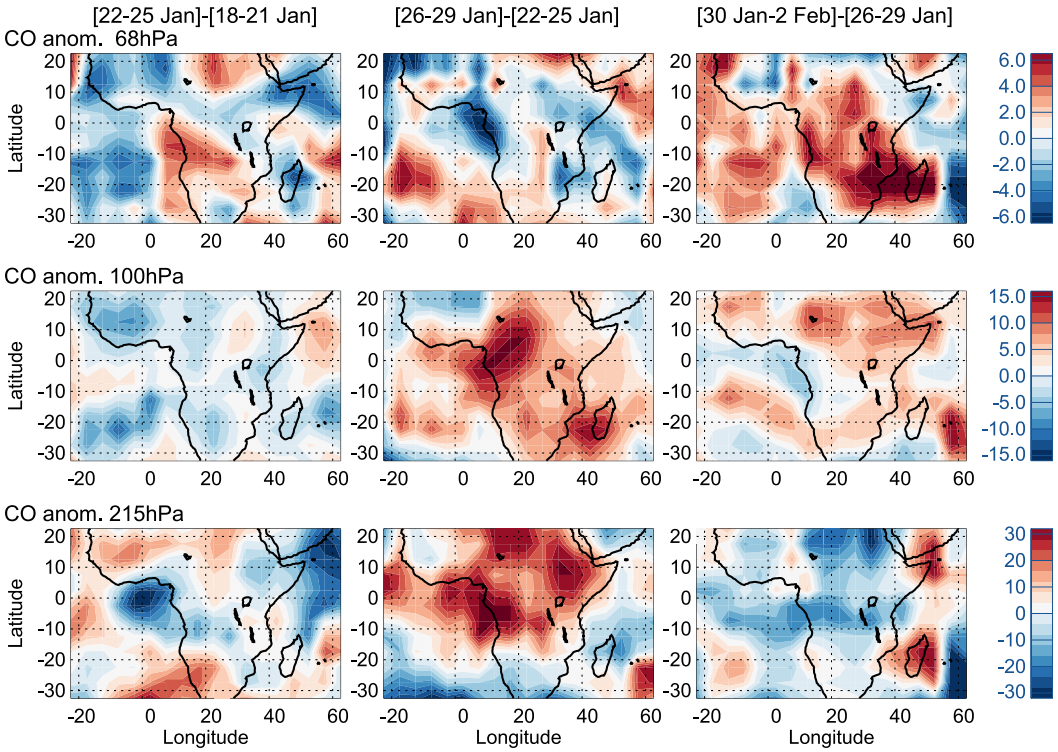

Fig. 5. Maps of CO differences at 68, 100 and 215 hPa for three periods: between 18–21 January and 22–25 January (left panels), between 22–25 January and 26–29 January (middle panels) and between 26–29 January and 30 January–2 February (right panels).

above 100 hPa increased and propagated downward from MS, modulating the negative O_3 gradient in regions with steep vertical gradient of O_3, such as TTL, and thus produced a dominant signature on the O_3 field in UT/LS.

As mentioned in Section 1, we discuss here the inter-annual variation of CO in LS. The time series of tropical (15°S−15°N) CO at 68 hPa (2004−2015) derived by EOS/MLS shows that high CO concentrations were recorded in BW (December to February) in 2005, 2006, 2010, and 2013 (e.g., Minschwaner et al. 2016). Figure 1 showed that the CO in the LS and stratospheric upwelling are well correlated in the 2010 BW. However, despite a major SSW in 2009, a high CO concentration was not recorded in the LS because the strength of the upward motion in the TTL and the location of deep convection were different (not over CO source region) from those in 2010 (not shown). We showed that the timing (related to the SSW occurrence) and location of enhanced convection and the relationship between convection and source region of the tracer (e.g., Africa for CO) are mutually important for the CO variation at LS (Fig. 1).

The inter-annual variation of CO in the LS is caused by influences from both the troposphere and stratosphere, such as the Madden-Julian Oscillation, the El Nino Southern Oscillation, and the QBO. It is suggested from the case study of 2010 SSW that the strength and location of the deep convection and the stratospheric upward motion in the tropics play an important role in the inter-annual variations of CO in TTL and LS, though a further investigation of this matter is beyond the scope of this paper.

Acknowledgments

The present work was partly supported by a JSPS Kakenhi Grant-in-Aid for Scientific Research (C), No.25340010, the Ministry of Education, Culture, Sports, Science and Technology and partly by the Program for Promoting the Enhancement of Research Universities at Kyushu University. The MHS data used in this study were provided by the NOAA FS Comprehensive Large Array Data Stewardship System (Data set: TOVS), and were obtained with support from the French INSU-CNES Mixed Service Unit ICARE via CLIMSERV-IPSL.

Edited by: T. Horinouchi

References

Abalos, M., W. J. Randel, and E. Serrano, 2012: Variability in upwelling across the tropical tropopause and correlations with tracers in the lower stratosphere. *Atmos. Chem. Phys.*, **12**, 11505−11517, doi:10.5194/acp-12-11505-2012.

Aschmann, J., B. M. Sinnhuber, E. L. Atlas, and S. M. Schauffer, 2009: Modeling the transport of very short-lived substances into the tropical upper troposphere and lower stratosphere. *Atmos. Chem. Phys.*, **9**, 9237−9247, doi:10.5194/acp-9-9237-2009.

Chaboureau, J. P., J. P. Cammas, J. Duron, P. J. Mascart, N. M. Sitnikov, and H.-J. Voessing, 2007: A numerical study of tropical cross-tropopause transport by convective overshoots. *Atmos. Chem. Phys.*, **7**, 1731−1740, doi:10.5194/acp-7-1731-2007.

Collimore, C. C., D. W. Martin, M. H. Hitchman, A. Huesmann, and D. E. Waliser, 2003: On the relationship between the QBO and tropical deep convection. *J. Climate*, **16**, 2552−2568, doi:10.1175/1520-0442(2003)016<2552:OTRBTQ>2.0.CO;2.

Dee, D. P., and co-authors, 2011: The ERA-Interim reanalysis: Configuration and performance of the data assimilation system. *Quart. J. Roy. Meteorol. Soc.*, **137**, 553−597, doi:10.1002/qj.828.

Eguchi, N., and K. Kodera, 2007: Impact of the 2002, Southern Hemisphere, stratospheric warming on the tropical cirrus clouds and convective activity. *Geophys. Res. Lett.*, **34**, L05819, doi:10.1029/2006GL028744.

Eguchi, N., and K. Kodera, 2010: Impacts of stratospheric sudden warming event on tropical clouds and moisture fields in the TTL: A Case Study. *SOLA*, **6**, 137−140, doi:10.2151/sola.2010-035.

Eguchi, N., K. Kodera, and T. Nasuno, 2015: A global non-hydrostatic model study of a downward coupling through the tropical tropopause layer during a stratospheric. *Atmos. Chem. Phys.*, **15**, 297−304, doi:10.5194/acp-15-297-2015.

Evan, S., K. Rosenlof, T. Thornberry, D. Rollings, and S. Khaykin, 2015: TTL cooling and drying during the January 2013 stratospheric sudden warming. *Quart. J. Roy. Meteor. Soc.*, **141**, 3030−3039, doi:10.1002/qj.2587.

Funatsu, B. M., V. Dubreuil, C. Claud, D. Arvor, and M. A. Gan, 2012: Convective activity in Mato Grosso state (Brazil) from microwave satellite observations: Comparisons between AMSU and TRMM data sets. *J. Geophys. Res. Atmos.*, **117**, D16109, doi:10.1029/2011JD017259.

Hong, G., G. Heygster, J. Miao, and K. Kunzi, 2005: Detection of tropical deep convective clouds from AMSU-B water vapor channels measurements. *J. Geophys. Res. Atmos.*, **110**, D05205, doi:10.1029/2004JD004949.

Kodera, K., 2006: Influence of stratospheric sudden warming on the equatorial troposphere. *Geophys. Res. Lett.*, **33**, L06804, doi:10.1029/2005GL024510.

Kodera, K., N. Eguchi, J. N. Lee, Y. Kuroda and S. Yukimoto, 2011: Sudden chgange in the tropical straospheric and tropopshperic Circulation during January 2009. *J. Meteor. Soc. Japan*, **89**, 283−290, doi:10.2151/jmsj.2011-308.

Kodera, K., B. M. Funatsu, C. Claud, and N. Eguchi, 2015: The role of convective overshooting clouds in tropical stratosphere-troposphere dynamical coupling. *Atmos. Chem. Phys.*, **15**, 6767−6774, doi:10.5194/acp-15-6767-2015.

Kopacz, M., and co-authors, 2010: Global estimates of CO sources with high resolution by adjoint inversion of multiple satellite datasets (MOPITT, AIRS, SCIAMACHY, TES). *Atmos. Chem. Phys.*, **10**, 855−876, doi:10.5194/acp-10-855-2010.

Livesey, J. N., W. G. Read, P. A. Wagner, L. Froidevaux, A. Lambert, G. L. Manney, L. F. Mill ‘an Valle, H. C. Pumphrey, M. L. Santee, M. J. Schwartz, S. Wang, R. A. Fuller, R. F. Jarnot, B. W. Knosp, and E. Martinez, 2015: Earth Observing System (EOS) Aura Microwave Limb Sounder (MLS) Version 4.2x Level 2 data quality and description document. JPL D-33509 (Available online at http://mls.jpl.nasa.gov/data/v4-2_data_quality_document.pdf, accessed on 1 June 2016).

Minschwaner, K., H. Su, and J. H. Jiang, 2016: The upward branch of the brewer-dobson circulation quantified by tropical stratospheric water vapor and carbon monoxide measurements from the aura microwave limb sounder. *J. Geophys. Res.*, doi:10.1002/2015JD023961, in press.

Ott, L., S. Pawson, and J. Bacmeister, 2011: An analysis of the impact of convective parameter sensitivity on simulated global atmospheric CO distributions. *J. Geophys. Res.*, **116**, D21310, doi:10.1029/2011JD016077.

Park, M., W. J. Randel, A. Gettelman, S. Massie, and J. Jiang, 2007: Transport above the Asian summer monsoon anticyclone inferred from Aura MLS tracers. *J. Geophys. Res.*, **112**, D16309, doi:10.1029/2006JD008294.

Randel, W. J., K. Zhang, and R. Fu, 2015: What controls stratospheric water vapor in the NH summer monsoon regions. *J. Geophys. Res. Atmos.*, **120**, 7988−8001, doi:10.1002/2015JD023622.

Schoerbal, M. R., A. R. Douglass, R. S. Stolarski, S. Pawson, S. E. Strahan, and W. Read, 2008: Comparison of lower stratospheric tropical mean vertical velocities. *J. Geophys. Res. Atmos.*, **113**, D05301, doi:10.1029/2008JD010221.

Ueyama, R., E. P. Gerber, J. M. Wallace, and D. M. W. Frierson, 2013: The role of high-latitude waves in the intraseasonal to seasonal variability of tropical upwelling in the Brewer–Dobson circulation. *J. Atmos. Sci.*, **70**, 1631−1648, doi:10.1175/JAS-D-12-0174.1.

Wang, T., W. J. Randel, A. E. Dessler, M. R. Schoeberl, and D. E. Kinnison, 2014: Trajectory model simulations of ozone (O_3) and carbon monoxide (CO) in the lower stratosphere. *Atmos. Chem. Phys.*, **14**, 7135−7147, doi:10.5194/acp-14-7135-2014.

Winker, D. M., W. H. Hunt, and M. J. Mcgill, 2007: Initial performance assessment of CALIOP. *Geophys. Res. Lett.*, **34**, D19803, doi:10.1029/2007GL030135.

Manuscript received 28 April 2016, accepted 26 June 2016
SOLA: https://www.jstage.jst.go.jp/browse/sola/